Using the STARS Model to Evaluate Effects of the Proposed Action on Juvenile Salmon Survival, Travel Time, and Routing for the Reinitiation of Consultation on the Coordinated Long-Term Operation of the Central Valley Project and State Water Project

By Russell W. Perry, Adam C. Pope, and Vamsi K. Sridharan

Prepared in cooperation with National Oceanic and Atmospheric Administration, National Marine Fisheries Service

Open File Report 2019–XXXX

U.S. Department of the Interior
U.S. Geological Survey

U.S. Department of the Interior
DAVID L. BERNHARDT, Secretary

U.S. Geological Survey
James Reilly II, Director

U.S. Geological Survey, Reston, Virginia: 2019

Suggested citation:
Perry, R.W., Pope, A.C., and Sridharan, V.K., 2019, Using the STARS Model to Evaluate Effects of the Proposed Action on Juvenile Salmon Survival, Travel Time, and Routing for the Reinitiation of Consultation on the Coordinated Long-Term Operation of the Central Valley Project and State Water Project: U.S. Geological Survey Open-File Report 2019-XXXX, XX p. plus appendixes, https://doi.org/10.3133/ofr2019xxxx.

ISSN 2331-1258 (online)

Contents

Figures

Conversion Factors

Inch/Pound to International System of Units

Multiply	By	To obtain
	Volume	
acre-foot (acre-ft)	1,233	cubic meter (m^3)
	Flow rate	
cubic foot per second (ft^3/s)	0.02832	cubic meter per second (m^3/s)

International System of Units to Inch/Pound

Multiply	By	To obtain
	Length	
kilometer (km)	0.6214	mile (mi)

Abbreviations

DCC	Delta Cross Channel
DSM-2	Delta Simulation Model 2
MCMC	Markov Chain Monte Carlo
COS	Continuing Operations
PA	Proposed Action
USGS	U.S. Geological Survey
WY	water year
WYI	water year index

Using the STARS Model to Evaluate Effects of the Proposed Action on Juvenile Salmon Survival, Travel Time, and Routing for the Reinitiation of Consultation on the Coordinated Long-Term Operation of the Central Valley Project and State Water Project

By Russell W. Perry[1], Adam C. Pope[1], Vamsi K. Sridharan[2]

Abstract

In 2016, the Bureau of Reclamation and California Department of Water Resources requested the reinitiation of consultation on the coordinated long-term operation of the Central Valley Project and State Water Project, resulting in a Biological Assessment released in 2019. In its analysis of the Biological Assessment for the Biological Opinion on the proposed action, the National Marine Fisheries Service requested our assistance to aid in understanding the effect of the proposed action on juvenile Chinook salmon (*Oncorhynchus tshawytscha*) populations migrating through the Sacramento-San Joaquin River Delta (henceforth, "the Delta"). Therefore, in this report we analyzed an 82-year time series of simulated river flows and Delta Cross Channel (DCC) gate operations under two scenarios constructed for the Biological Assessment: the proposed action scenario (PA) and the continuing operations scenario (COS).

To evaluate the proposed action, we used the STARS model (Survival, Travel time, And Routing Simulation model), a stochastic, individual based simulation model designed to predict survival of a cohort of fish that experience variable daily river flows as they migrate through the Delta. The STARS model used parameter estimates from a Bayesian mark-recapture model that jointly estimated travel time and survival in eight discrete reaches of the Delta and migration routing at two key river junctions.

By applying the STARS model to the two 82-year scenarios, we found that the proposed action had negative effects on survival, travel time, and routing in October–December but positive effects in April–June. In November-December, there was a high probability that survival for PA was less than COS and that travel time and routing to the Interior Delta for PA was greater than COS. We identified that magnitude of the difference in survival between scenarios was large in some years. For example, we quantified that survival under the PA scenario was 10 percentage points lower than COS in 25% of the water years in October–December. During this period, inflow to the Delta tended to be lower under the PA scenario and the DCC gate was open more frequently under the PA scenario relative to the COS scenario. Lower inflow reduced survival and more frequent operation of the DCC 1) increased the proportion of fish entering the Interior Delta where survival was low, and 2) reduced survival in the Sacramento River in reaches downstream of the DCC. In contrast, during April-June

---

[1]U.S. Geological Survey
[2]University of California, Santa Cruz

survival was higher, travel times were lower, and routing to the Interior Delta was lower under the PA scenario relative to COS, although the magnitude of increase was relatively small in most years (less than a 3-percentage point difference in survival). This difference between scenarios was driven by higher river flows in some years under the PA scenario relative to COS.

Introduction

The U.S. Bureau of Reclamation (Reclamation) and California Department of Water Resources (DWR) has responsibility for the coordinated long-term operations of the Central Valley Project (CVP) and State Water Project (SWP). The CVP and SWP are a system of dams, rivers, and water conveyance structures with the purposes of generating power and delivering water for agricultural and domestic use while providing flood protection and protecting water quality for downstream users (Reclamation, 2019). Because the Sacramento and San Joaquin watersheds harbor several critically endangered species listed under the Endangered Species Act (ESA), Reclamation has undergone ESA consultation with the U.S. Fish and Wildlife and National Marine Fisheries Service (NMFS). Most recently, NMFS issued a Biological Opinion in 2009 (NMFS, 2009) concluding that the long-term operations of the CVP and SWP were likely to jeopardize the continued existence of Sacramento River Winter-Run Chinook Salmon, Central Valley Spring-Run Chinook Salmon, California Central Valley Steelhead (*Oncorhynchus mykiss*), Southern distinct population segment (DPS) of North American Green Sturgeon (*Acipenser medirostris*), and Southern Resident DPS of Killer Whale (*Orcinus orca*). In 2016, Reclamation and DWR requested the reinitiation of consultation on the coordinated long-term operation of the CVP and SWP, resulting in a Biological Assessment released in 2019 (Reclamation, 2019).

The Biological Assessment described a proposed action that focused on a core water operation that would allow operation of the CVP and SWP for water supply and other project purposes, while also avoiding jeopardy of ESA-listed species. In its analysis of the Biological Assessment for the Biological Opinion on the proposed action, NMFS requested our assistance to aid in understanding the effect of the proposed action on juvenile Chinook salmon (*Oncorhynchus tshawytscha*) populations migrating through the Sacramento-San Joaquin River Delta (henceforth, "the Delta"). Over the past decade, the USGS has developed detailed statistical analyses of juvenile salmon acoustic telemetry data to understand how river flow, tides, and Delta Cross Channel (DCC) gate operations interact to affect migration routing and survival of juvenile Chinook salmon migrating through the Delta. Therefore, in this report we analyzed an 82-year time series of simulated river flows and DCC gate operations under two scenarios constructed for the Biological Assessment: the proposed action scenario (PA) and the continuing operations scenario (COS).

Our analysis made use of a Bayesian mark-recapture model that jointly estimated reach-specific travel time, migration routing, and survival of juvenile Chinook salmon. Statistical methods for this analysis are described in detail in Perry and others (2018). This model extended the work of Perry and others (2010) to estimate the effect of the Delta Cross Channel (see C_4 in fig. 1) and Delta inflows as measured in the Sacramento River at Freeport (U.S. Geological Survey [USGS] streamgage 11447650; see A_2 in fig. 1) on survival, routing, and travel time of juvenile Chinook salmon in eight reaches of the Delta (fig. 1). Perry and others (2018) determined that median travel time was related to inflow in all reaches of the Delta, but that survival was strongly related to inflow in only three reaches that transitioned from tidally influenced, bidirectional flow at low inflows to unidirectional downstream flow as inflows increased. These three reaches caused overall route-specific survival through the Delta to increase with flow, yet fish that entered the interior Delta (reach 8 in fig. 1) through Georgiana Slough or the DCC had lower survival than through other migration routes. Overall survival decreased further through lower survival of fish entering the interior Delta through Georgiana Slough or the DCC, combined with a higher proportion of fish entering the interior Delta as inflows decreased to less than about 25,000 ft^3/s and when the Delta Cross Channel gate was opened (Perry and others, 2018).

Although the effect of river flow on overall survival through the Delta has been established for some time (Newman and Rice, 2002; Newman, 2003; Perry, 2010), our goal was to use the recently developed survival, travel time, and routing relationships (Perry and others, 2018) to better understand the potential magnitude of the effect of the proposed action on juvenile salmon survival, routing, and travel time. Because our model incorporated the effect of river flow and DCC gate operation on routing, travel time, and survival, our analysis can identify mechanisms for how operations affect overall survival through the Delta. One drawback, however, is that the statistical model of Perry and others (2018) did not include water exports (i.e., pumping water out of the Southern Delta). Thus, the modeling results in this report are insensitive to any difference in exports between scenarios. Although we are currently developing models that include export effects, those models were not available in time to use for this analysis.

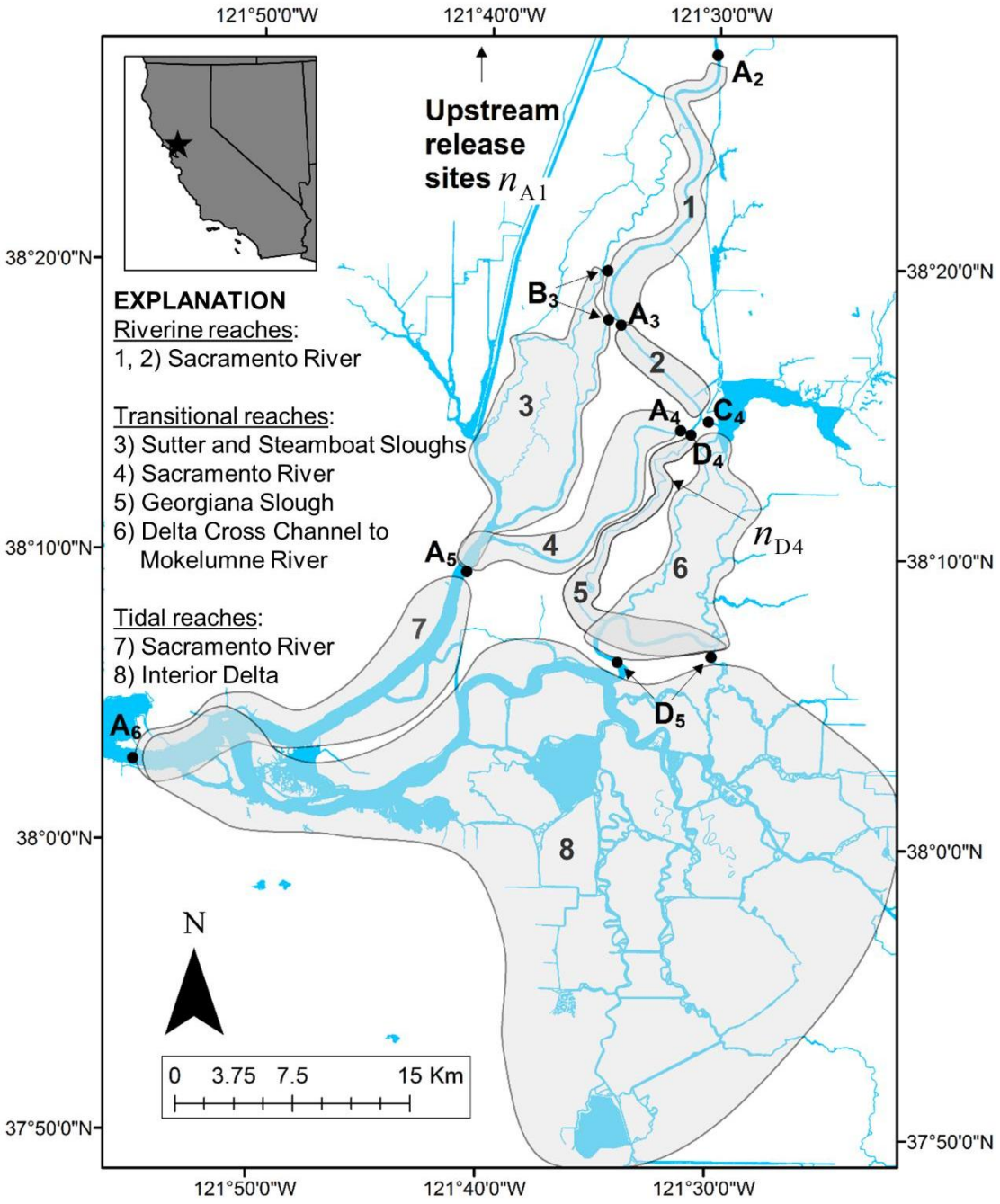

Figure 1. Map showing location of acoustic telemetry receiving stations (filled black circles) used to detect acoustic-tagged juvenile Chinook salmon as they migrated through the Sacramento-San Joaquin River Delta, northern California. Telemetry stations are labeled by migration route (A, Sacramento River; B, Sutter and Steamboat Sloughs; C, Delta Cross Channel; D, Georgiana Slough) and sampling occasion (1–7). These telemetry stations divide the Delta into eight discrete reaches (shown by numbered shaded regions), with an additional reach upstream of telemetry station A_2 (Reach 0) used as an acclimation reach to allow fish to recover from post-release handling. Route-specific survival begins at A_2 (Freeport) and ends at A_6 (Chipps Island). Release sites are labeled as n_{A1} and n_{D4}.

Methods

Model Description

Here we provide a summary of the STARS model and the associated Bayesian mark-recapture model we used to simulate survival, travel time, and migration routing. STARS stands for Survival, Travel time, And Routing Simulation, a stochastic, individual based simulation model designed to predict survival of a cohort of fish that experiences variable daily river flows as they migrate through the Delta.

Summary of the Bayesian Mark-Recapture Model Output

The STARS model uses parameter estimates from a Bayesian mark-recapture model that jointly estimates travel time and survival in eight discrete reaches of the Delta and migration routing at two key river junctions (fig. 1). The data for the analysis consisted of 2,170 acoustic-tagged late-fall Chinook salmon released during a 5-year period (2007–11) over a wide range of Sacramento River inflows (6,816–76,986 ft^3/s at Freeport). This analysis was based on acoustic telemetry data from several published studies where details of each study are available (Perry and others, 2010, 2013; Michel and others, 2015).

Although numerous studies have identified a relation between Delta inflows and survival at the Delta-wide scale, the goal of the Perry and others (2018) analysis was to quantify how the flow-survival relation varied spatially among different regions of the Delta. To quantify the reach-specific relation between river inflows and survival, the analysis used time-varying individual covariates where an individual's covariate value was defined as the flow of the Sacramento River at Freeport and the DCC gate position on the day that *i*th fish entered the *m*th reach. Owing to missing covariate values for undetected fish, the analysis implemented the multistate mark-recapture model of Perry and others (2010) using a complete data likelihood approach in a Bayesian framework (King and others, 2010). To account for missing covariate values, the analysis jointly modeled reach-specific travel times, routing, and survival. Estimated parameters of a log-normal travel time distribution for each reach were used to impute travel times of undetected fish, which in turn allowed missing covariate values to be defined based on the imputed arrival time in a given reach. Markov Chain Monte Carlo (MCMC) techniques were used to integrate over the missing covariate values by drawing missing travel times on each iteration of the Markov chain.

The analysis found that the proportion of fish using each migration route depended on river flow, but the direction of the relationship differed among river junctions (fig. 2). At the junction of the Sacramento River with Sutter and Steamboat Sloughs (B_3 in fig. 1), the probability of fish entering Sutter and Steamboat sloughs increased with river flow. In contrast, at the junction of the Sacramento River with Georgiana Slough (D_4 in fig. 1) and the DCC (C_4 in fig. 1), the probability of fish entering Georgiana Slough decreased with increasing flow. Opening the DCC gates decreased the probability of entering Georgiana Slough but increased the total proportion of fish entering the Interior Delta via both the DCC and Georgiana Slough.

The analysis of Perry and others (2018) also identified a relation between river inflows and median travel times in all reaches of the Delta (fig. 4). In contrast, the flow-survival relation among reaches varied considerably (fig. 3). In the upper reaches of the Delta (reaches 1 and 2 in fig. 1), survival was consistently high regardless of inflows, whereas in the strongly tidal reaches (reaches 7 and 8 in fig. 1), there was no significant relation between river inflows and reach-specific survival despite a relation between inflow and travel time. The strongest flow-survival relations were identified in the three reaches that transition from river-dominated to tidally dominated flows (reaches 3, 4, and 5 in fig. 1).

The product of reach-specific survival for a given migration pathway between Freeport (A_2 in fig. 1) and Chipps Island (A_6 in fig. 1) yields the probability of surviving through each migration route at a given river discharge. Route-specific survival for all routes increased with river discharge but approached an asymptote, leveling off at about 0.75 for the Sacramento River and Sutter and Steamboat Sloughs, and at about 0.35 for fish entering Georgiana Slough when river discharges increase to more than 30,000–40,000 ft^3/s (fig. 4). The reach-specific survival relations indicate that the asymptote in route-specific survival was driven by the survival in the strongly tidal reaches (reaches 7 and 8) since survival for all other reaches approached 1 as flow increased but remained constant with flow for the strongly tidal reaches. Expected travel time distributions through each migration route decreased as river flow increased, with migration routes leading to the interior Delta (Georgiana Slough and the Delta Cross Channel) having longer travel times than other routes (fig. 5).

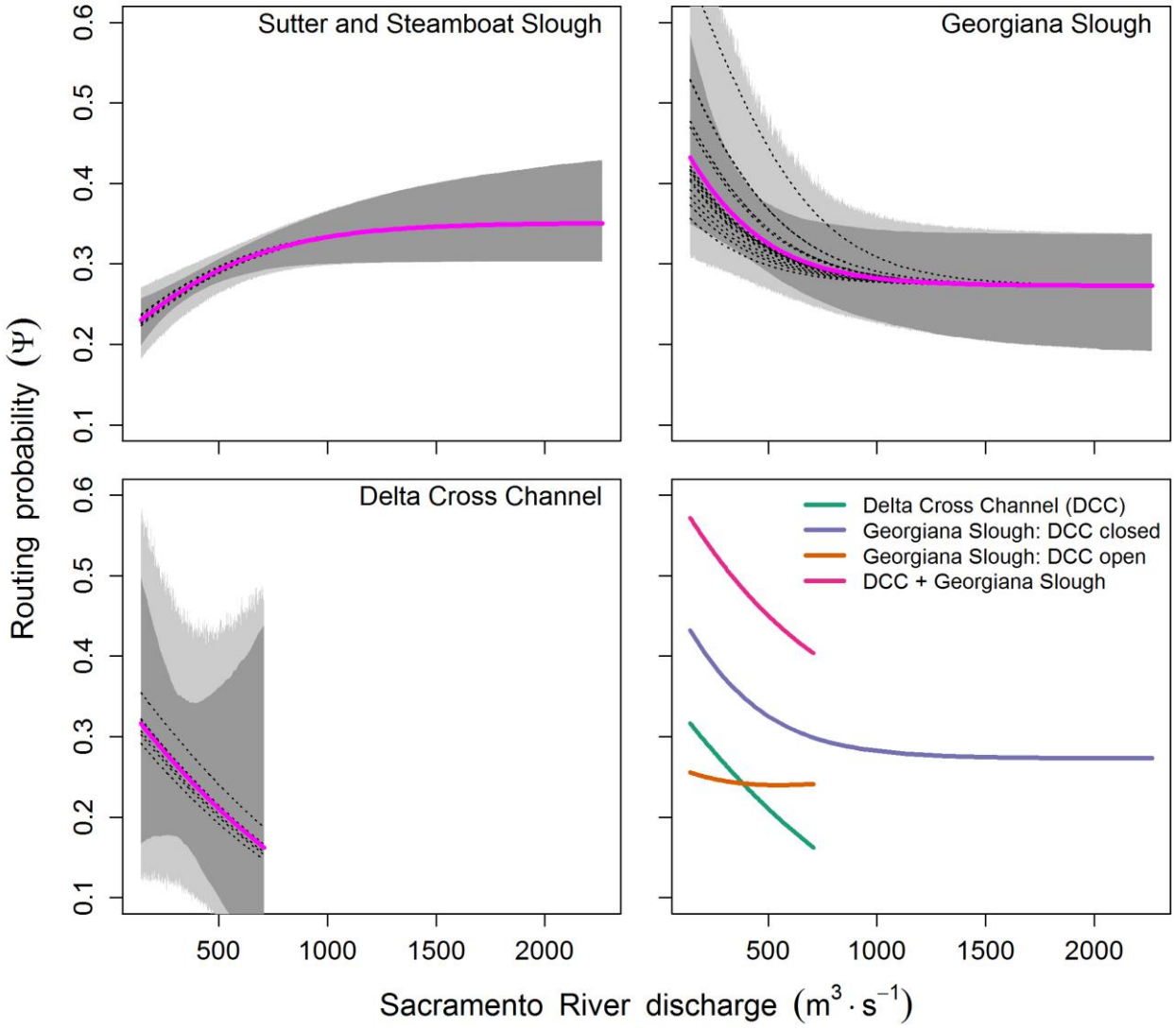

Figure 2. Relationships between routing probability and inflow to the Delta as measured at the Sacramento River at Freeport (A2 in Fig. 1). The lower right panel shows the effect of Delta Cross Channel (DCC) gate position on routing probabilities at the junction of the Sacramento River, Delta Cross Channel, and Georgiana Slough (A4, C4, and D4 in Fig. 1), plotted at the posterior median of the parameters. Other panels show mean routing relationships (heavy magenta line), random effects estimates for each release group (dotted lines), 95% credible interval about the mean relationship (dark gray region), and 95% confidence interval among release groups (light gray region).

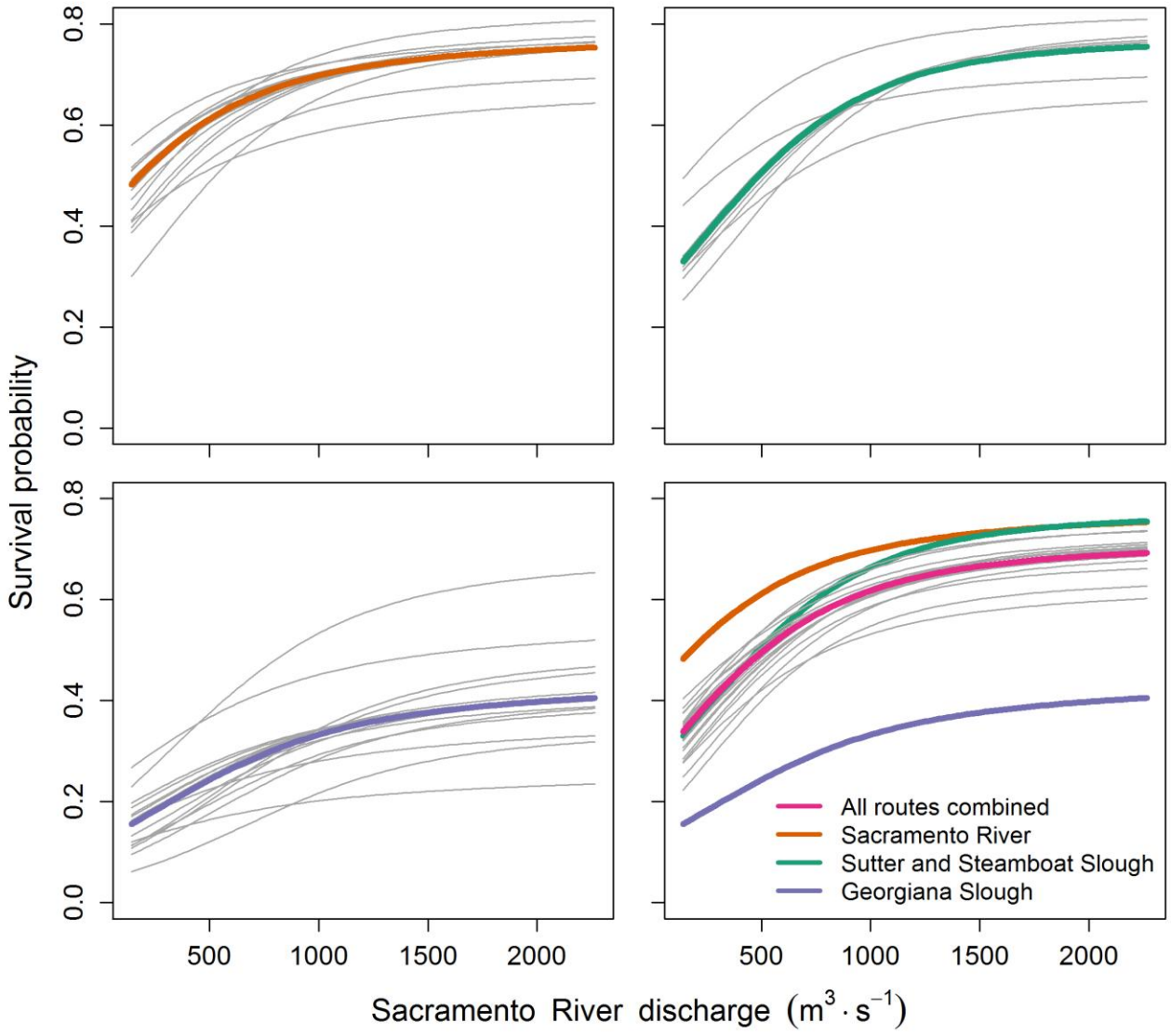

Figure 3. Graphs showing route-specific survival of juvenile Chinook salmon between Freeport and Chipps Island (see fig. 1), through the Sacramento-San Joaquin River Delta, northern California. Route-specific survival based on posterior median parameter values was calculated as the product of reach-specific survival for reaches that trace each unique migration route through the Delta (shown for closed Delta Cross Channel gates). Top graphs and bottom left graph show the mean relation for each route, with thin gray lines showing the random effect estimates for each release group. Bottom right graph compares the route-specific survival relations and includes all routes combined. ft^3/s × 1,000, thousands of cubic feet per second.

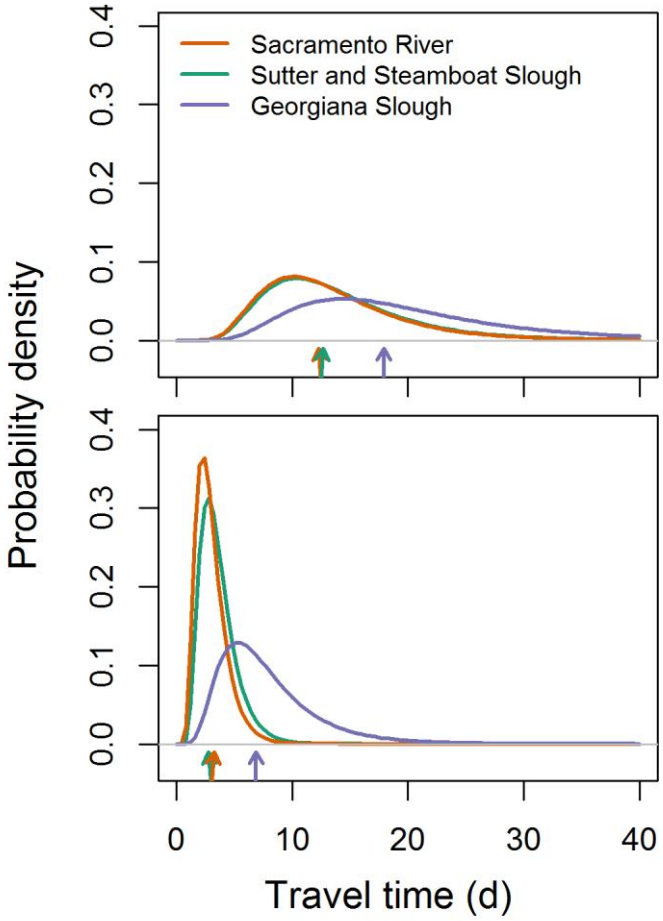

Figure 4. Graphs showing route-specific travel time distributions of juvenile Chinook salmon at the 5th (top graph) and 95th (bottom graph) percentiles of discharge based on the historical flow record (8,290 and 47,910 ft^3/s), between Freeport and Chipps Island (see fig. 1), Sacramento-San Joaquin River Delta, northern California. Graphs were based on posterior medians of parameters for reach-specific travel time distributions assuming closed Delta Cross Channel gates. d, days; ft^3/s, cubic foot per second.

STARS: Survival, Travel Time, and Routing Simulation

To simulate survival, travel time, and routing, we used the results from the Bayesian mark-recapture model of Perry and others (2018). To incorporate measures of uncertainty in our simulations, we used the joint posterior distribution of the survival, routing, and travel time parameters from the Bayesian analysis. Uncertainty was propagated by doing one simulation for each MCMC draw forming the joint posterior distribution of the parameters.

Random-effect terms in this model estimated the deviation of each release cohort from the average survival, routing, and travel time relations. However, because we were interested in simulating new cohorts of fish, we drew new random effects for each posterior draw from a normal distribution with mean 0 and standard deviations of ξ_S, ξ_Ψ, and ξ_μ (see Perry and others, 2018, for more detail). In this way, each draw of the joint posterior distribution represents a possible state of nature for how river flow and DCC gate operations affect travel time, routing, and survival of a given cohort of fish. When comparing alternative scenarios (for example, PA and COS), we used the same set of random effect draws for both scenarios because we envisioned that the same cohort of fish was migrating through the Delta, but under two possible alternative operational scenarios.

Given a daily time series of river flow and DCC gate operations the STARS model simulates survival, routing, and travel time as follows:

1. Select parameter set *i* from the joint posterior parameter distribution.
2. Initiate the simulation with 1,000 fish at Freeport on day *t*.
3. Calculate survival in reach 1 given discharge on day *t* and parameter set *i*.
4. Draw individual travel times through reach 1 from a lognormal distribution where the mean of the distribution depends on parameter set *i* and discharge on day *t* (eq. 2). This yields a distribution of individual arrival times at the junction of Sutter and Steamboat Sloughs and the Sacramento River (A_3 and B_3 in fig. 1).
5. Draw the route taken by each fish from a Bernoulli distribution where the probability of entering Sutter and Steamboat Sloughs is a function of parameters set *i* and discharge on the day each fish arrives at the junction.
6. Calculate the survival probability of each individual for the next reach downstream (Sacramento River or Sutter and Steamboat Sloughs) given discharge on the day each fish entered the reach.
7. Draw travel times for each individual for the next downstream reach given the flows on the day each fish entered the reach.
8. For fish remaining in the Sacramento River, draw the route taken by fish at the junction of the Sacramento River with the DCC and Georgiana Slough (A_4, C_4, and D_4 in fig. 1) from a multiple Bernoulli distribution where the probability of entering each route depends on the position of the DCC gates discharge on the day each fish arrived at the junction.
9. Repeat steps 4 and 5 for all remaining reaches.
10. Repeat steps 2–9 for all days in the daily time series.
11. Repeat steps 1–10 for all iterations of the joint posterior distribution.

This simulation yielded a posterior predictive distribution of reach-specific survival probabilities, reach-specific travel times, and routing probabilities for a cohort of 1,000 individuals entering the Delta at Freeport on each day of a daily time series. By using this approach, our simulation emulated the effect of daily flow variation on through-Delta survival, routing, and travel time for a cohort of fish that entered the Delta on a given day. For example, although two cohorts may enter the Delta under identical flows at Freeport, survival and travel time of these cohorts would differ if one cohort entered during an ascending hydrograph and another cohort entered during a descending hydrograph. To see an implementation of the STARS model, we encourage readers to visit NOAA's Central Valley Acoustic Tagging Website where the STARS model is currently being used to simulate travel time, survival, and routing in real-time for the current water year (https://oceanview.pfeg.noaa.gov/shiny/FED/CalFishTrack/).

Comparing the Proposed Action and Continuing Operations Scenarios

To understand the effect of the proposed action on survival, routing, and travel time of juvenile late-fall Chinook salmon, we simulated travel time, survival, and migration routing using an 82-year time series of river flows and DCC gate operations simulated under each scenario. Monthly river flows and DCC gate operations were simulated using the CalSim water operations model, and then disaggregated to daily river flows and gate operations for inputs into the Delta Simulation Model 2 (DSM-2), a one-dimensional branching hydrodynamic model of the Delta. For more details on how the simulated river operations were constructed, interested readers should consult the Biological Assessment (Reclamation, 2019). Because our model relied on daily inflows to the Delta and daily DCC gate operations, we used the daily river flows and DCC gate operations constructed as inputs for

DSM-2 for input to the STARS model. The STARS model produced through-Delta survival, migration routing, and travel time distributions for a cohort of fish entering the Delta at Freeport on each day of the 82-year daily time series for each scenario.

We summarized the simulation output to provide useful statistics describing each daily cohort:

- The daily proportion of fish using each unique migration route.
- The daily proportion of fish entering the Interior Delta via the DCC and Georgiana Slough.
- Overall survival through the Delta, calculated as the mean survival over all individuals that entered the Delta on day *t*. Because routing for each individual was randomly drawn at each river junction, the mean survival is weighted by the proportion of fish that used each route.
- Median travel time over all routes for individuals that entered the Delta on day *t*. Median travel time was calculated by first summing reach-specific travel times for each individual between Freeport and Chipps Island and then taking the exponent of the mean of the logarithm of travel times.

To display model output, we generated annual graphs of:

- Daily flows for each scenario,
- Daily overall through-Delta survival (S_{Delta}) and median travel time,
- Daily routing probabilities, and
- The difference between scenarios in S_{Delta}, median travel time, and the proportion of fish entering the Interior Delta.

For these graphs, we plotted the posterior medians and 80% credible intervals on the difference between scenarios. We selected two water years to present in the body of the report to represent model output; graphs for all 82 years are provided in appendixes 1–4.

To summarize the 82-year time series, we used boxplots to examine the probability of a difference and the magnitude of the difference in the daily survival, travel time between scenarios, and routing to the Interior Delta. For survival, we calculated the probability that survival for the PA scenario was less than for the COS scenario. This probability was calculated as the fraction of the posterior distribution of the daily difference in survival between scenarios that was less than 0. For travel time and routing to the Interior Delta, we calculated the probability that travel time or routing for the PA scenario was greater than under the COS scenario. This approach produced a daily time series of probabilities for the 82-year simulation, which we summarized using boxplots for each day of the year.

To examine the magnitude of the difference in survival, travel time, or routing to the Interior Delta, we used boxplots to display the distribution of posterior median differences for all years combined and by water-year type. DWR uses five classifications for water year type in the Sacramento Valley that are based on water year index value (WYI) in millions of acre-feet (MAF):

1. W=Wet, WYI greater than or equal to (≥)9.2;
2. AN=Above Normal, 7.8 less than or equal to (≤)WYI≤9.2;
3. BN=Below Normal, 6.5≤WYI≤7.8;
4. D=Dry, 5.4≤WYI≤6.5; and
5. C=Critical, WYI≤5.4 (Kapahi and others, 2006).

Results and Discussion

We show detailed survival, travel time, and routing results for two water years—WYs 1979, a below-normal water year, and 1990, a critically dry water year. We first focus on describing river

flows and gate operations. For both water years, we noticed sharp monthly "steps" in simulated daily river discharge, which is quite different than actual river flows (figs. 5 and 6). The steps are also apparent in most other years (Appendix 1). The disaggregation from monthly to daily data involved using splines to transition from one month to the next to prevent model instabilities, thereby preserving the pattern of monthly steps in river flows (personal communication, 9 May 2019, Steve Micko, Jacobs Engineering Group).

In WY 1979, 1990, and other water years (Appendix 1), we noticed differences in DCC gate operation during the October–December period. Although both the PA and COS scenario operated under the same DCC control rule, different flows for each scenario triggered DCC gate closures differently between scenarios. In CalSim, the number of days each month with the DCC gate closed between October and December 14 is determined by an empirical relationship between monthly average flow and the number of days per month that the flow at Wilkins Slough would be greater than 7,500 ft^3/s (ICF International, 2016). Because the specific days of gate closure in each month are not specified by CalSim, DSM-2 is structured to have gate openings occur on consecutive days in the beginning of each month and closures occur at the end of each month (see figs. 5 and 6 as examples). For example, in 1979, lower Delta inflows at Freeport during November under the PA scenario compared to the COS scenario are likely associated with lower flows at Wilkins Slough, thereby triggering fewer gate-closure days, allowing the DCC to remain open longer under the PA scenario relative to the COS scenario (fig. 5).

For WY 1979, through-Delta survival under the PA scenario was considerably lower than the COS scenario during October–November, owing to differences in discharge and operation of the DCC (fig. 5). During this period, the largest difference in survival (about 14 percentage points) occurred during mid-November, when the DCC was open under PA but closed under the COS and when discharge for PA was lower than COS. Patterns in travel time through the Delta were the opposite of patterns in survival, with longer median travel times under the PA scenario during October–November (fig. 7). Owing to both differences in flow and DCC operation, a higher proportion of fish entering the interior Delta via Georgiana Slough and the DCC under the PA scenario as compared to COS (figs. 9 and 11). In contrast, for 1990, the critically dry year, discharge and DCC operation were similar in October–December, leading to little differences in survival (fig. 6), travel time (fig. 8), or routing (figs. 10 and 12).

For WY 1979, differences in through-Delta survival between scenarios were caused by (1) the underlying flow survival relationships, (2) differences in survival among routes, and (3) differences in routing that shifted fish between high- and low-survival routes. For example, under the PA scenario during October–November, simulations indicated that a high proportion of fish entered the DCC (fig. 9) relative to COS, which increased the proportion of fish experiencing low survival and increased travel times (fig. 30). Lower flows under the PA relative to COS further increased the proportion of fish entering the Interior Delta (fig. 11), which exposed a higher fraction of fish to lower survival in the Interior Delta (fig. 3). Third, an open DCC gate reduced flows in the Sacramento River downstream of the DCC, reducing survival of salmon that remain in the Sacramento River (Perry and others, 2018).

For both WY 1979 and 1990, survival was slightly higher under the PA scenario in April-June owing to higher flows under the PA relative to COS (figs 5 and 6). During this period, higher flows reduced travel times (figs. 7 and 8) and slightly reduced entrainment into the Interior Delta (figs. 11 and 12). During the remainder of the year (January–April) there was essentially no difference in river flow or DCC gate operation, leading to no difference in survival, travel time, or routing (figs. 6–12). Detailed graphs for each water year are available in online appendices and indicated similar seasonal patterns as for WYs 1979 and 1990 (appendices 1–4).

Summaries of the 82-year simulation indicated consistent seasonal patterns between scenarios, reflecting seasonal differences in operation under each scenario. The simulations indicated a median

probability near one that survival for the PA scenario was less than the COS scenario between mid-October and late November (fig. 13). In mid-November, the 25th percentile was about 0.8 indicating that 75% of the years had an 80% probability or greater that survival under the PA was less than COS. Similar patterns occur with travel time (fig. 14) and routing (fig. 15) during this period. In contrast, during May–mid-June, there was a very low probability of survival under PA being less than COS, owing to tendency for survival to be higher under PA relative to COS. For example, the median probability was near zero, indicating a very low probability of survival under PA being less than COS in half the years. In mid-May, the 75% percentile was about 0.1, indicating 75% of water years had a 10% probability or less that survival under PA was less than COS. Similar patterns occur with travel time (fig. 14) and routing (fig. 15) during this period. For January – April, there was very little difference in survival, travel time, or routing to the interior Delta.

Boxplots of the median difference between scenarios indicated seasonal patterns in the magnitude of the difference in survival, routing, and travel time. During mid-October–mid-November, the median survival differences between the PA and COS was about 0.02 (fig. 16). Although the median difference was small, the 25th percentile approached -0.10 in early November, indicating that survival under the PA scenario was more than 10 percentage points lower than the COS scenario in 25% of water years. Similar patterns occur with median travel time (fig. 17) and routing into the Interior Delta (fig. 18), except in the opposite direction of survival. For mid-April–June, the 25th percentile of survival differences between scenarios was about zero, indicating that survival under the PA was higher than under COS in 75% of years (fig. 16). However, the 75th percentile of survival differences was less than 0.03, indicating a small increase in survival in most years (fig. 16). Travel time (fig. 17) and routing to the Interior Delta (fig. 18) showed similar patterns as survival for mid-April–June, but in the opposite direction of survival.

The difference in survival (fig. 19), travel time (fig. 20), and routing (fig. 21) between scenarios varied among water year types and season. In October–December, survival differences were similar among water year types except under critically dry years when there was less of a difference in survival between scenarios. In contrast, in April–June, wet and above normal years exhibited lower differences in survival between scenarios relative to below normal, dry, and critical years (fig. 19). Similar patterns among water year type were evident with travel time (fig. 20) and routing to the Interior Delta (fig. 21).

Although our analysis with the STARS model provides insight about potential effects of the proposed action on juvenile salmon migrating through the Delta, there are several important limitations and assumptions that affect inferences drawn from the model. First, the sole drivers of survival, routing, and travel time in our model are DCC gate position and mean daily inflow to the Delta measured on the Sacramento River at Freeport. Thus, the results we present here are insensitive to other factors that might influence survival and that could differ between scenarios, such as water exports from the Delta (Newman and Rice, 2002; Newman, 2003; Newman and Brandes, 2010). Second, care should be taken when extending inferences beyond the range of data used to fit the model. Observed flows for the analysis conducted by Perry and others (2018) encompassed the 1st–95th percentiles of historical flow, bolstering inferences from the model about the effect of inflows. Third, the model was fit to large hatchery-origin late-fall Chinook salmon smolts that migrated through the Delta during December–March, yet here we are extending inferences to all runs over the entire migration period. Thus, survival of other runs at other times of year could have a different response to operations under the proposed action. Last, because our model was fitted to juvenile salmon telemetry data during 2005–11, it is a representation of the Delta in its current state, not some future state. Because our model characterized the relation between Delta inflows and survival in the present-day Delta, our model would be insensitive to future changes to the Delta that modify the relation between inflows and survival. For example, Perry and others (2018) identified the strongest flow-survival relations in reaches that transitioned from bidirectional tidal flows at low inflows to unidirectional

river flow at high inflow, implicating the tides as an important driver of the flow survival relation. Future sea level rise due to climate change would alter tidal dynamics in the Delta, which in turn could modify the relation between inflow and survival. Our model is insensitive to these types of changes to a future Delta.

Given these caveats, our analysis was able to (1) provide a comprehensive assessment of the proposed action by quantifying relative changes in key population metrics between scenarios, (2) identify the magnitude of these changes at given inflows and given times of the year, and (3) shed light on the mechanisms driving differences between scenarios. Ultimately, these analyses and others done for the Biological Opinion on the coordinated long-term operations of the SWP and CVP will help to develop system operations that minimize effects on listed species while allowing for water use to benefit the State of the California and the nation.

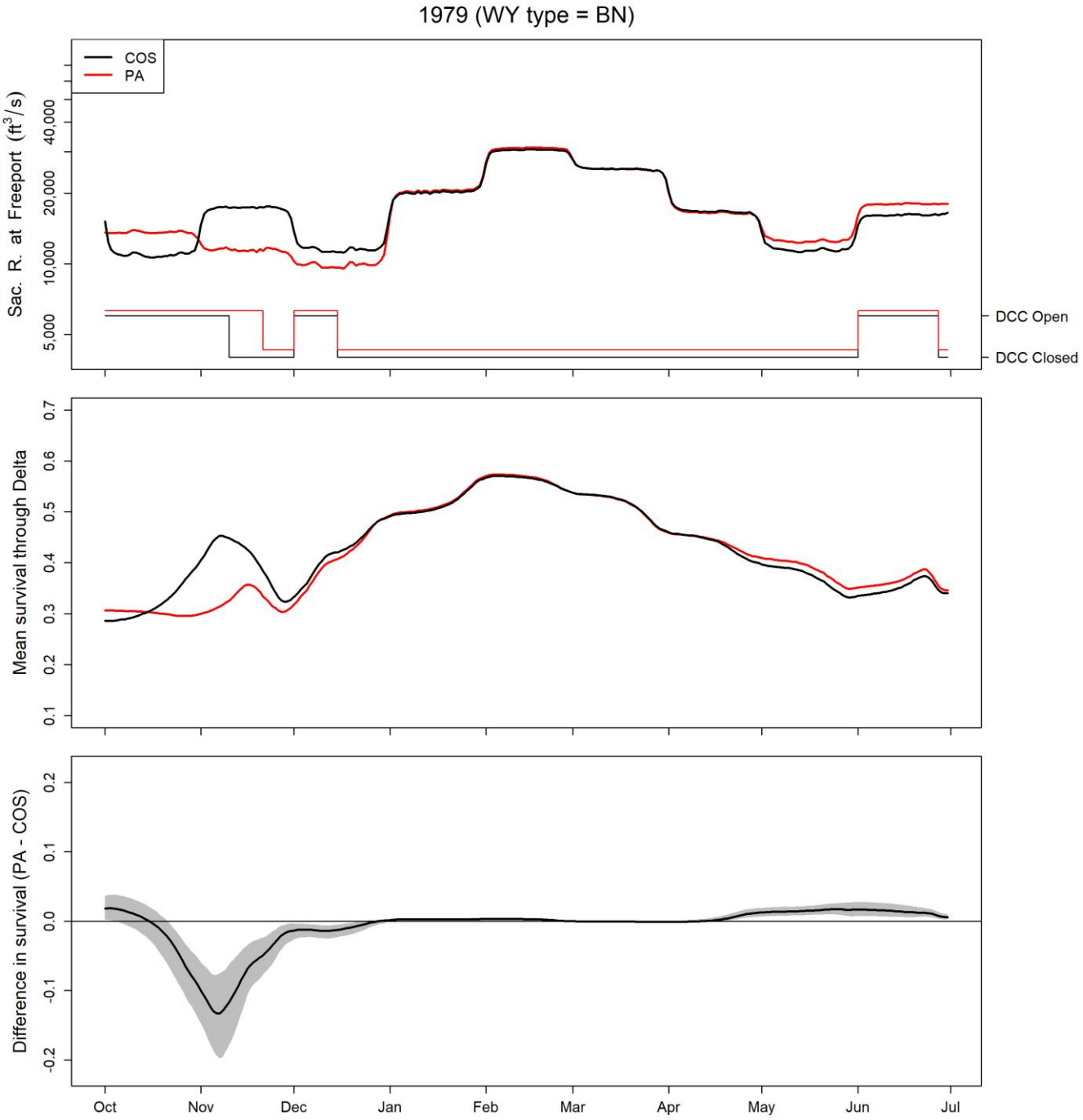

Figure 5. Graphs showing simulated daily bypass flows and Delta Cross Channel (DCC) gate operations for water year 1979 (top graph), median of simulated mean daily survival through the Sacramento-San Joaquin River Delta, northern California (middle graph), and the difference in survival between the Proposed Action (PA) and No Action Alternative (NAA) scenarios (bottom graph). Heavy lines in the top graph show bypass discharge on the primary y-axis, and thin lines show DCC operation of open or closed on the second y-axis. In the bottom graph, the gray shaded region shows the 90% credible interval on the difference in survival between scenarios. Discharge in the top graph is shown on a logarithmic scale to highlight variation in discharge when discharge is low. BN, Below Normal; WY, water year; ft^3/s, cubic foot per second; -, minus.

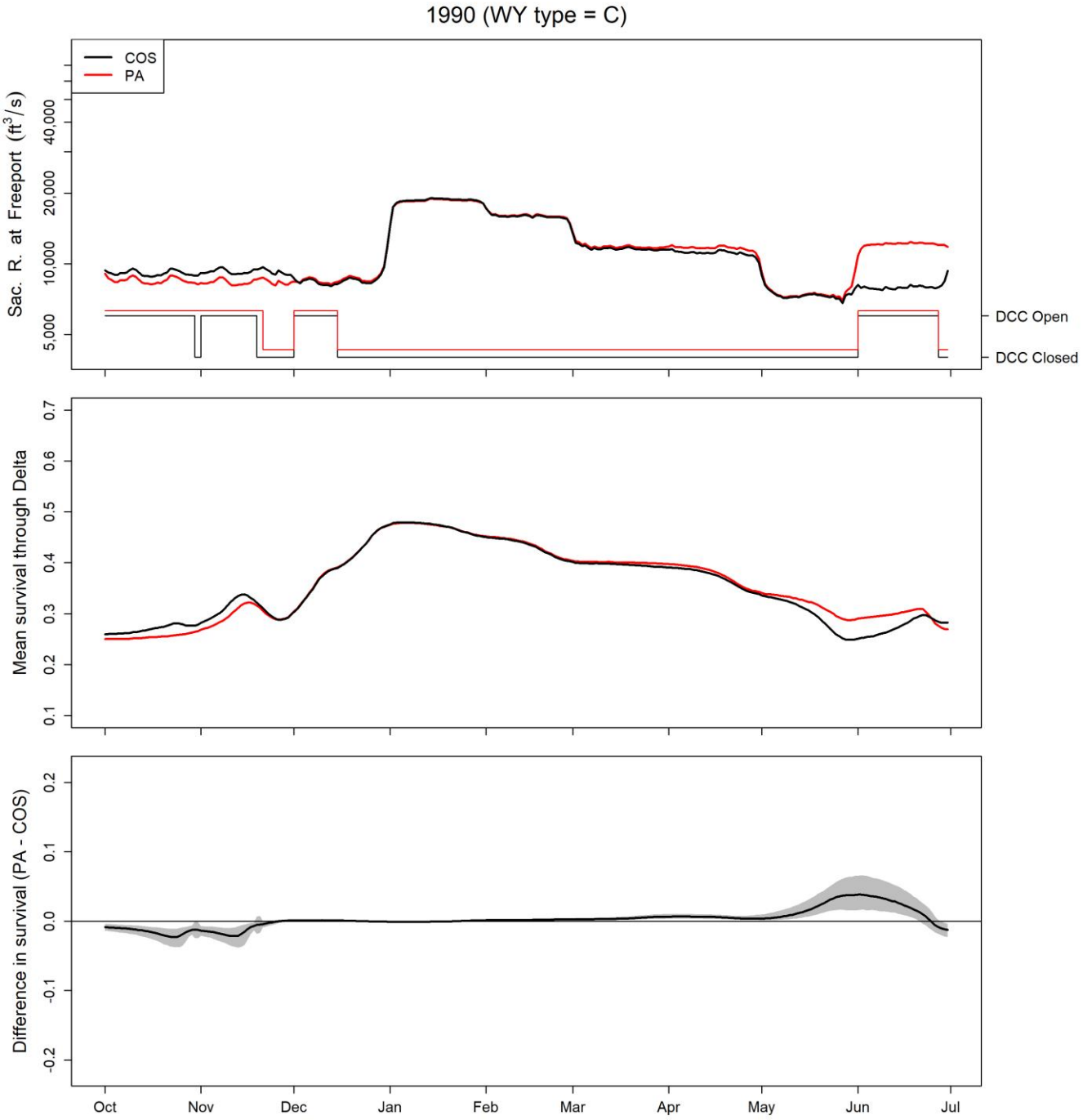

Figure 6. Graphs showing simulated daily bypass flows and Delta Cross Channel (DCC) gate operations for water year 1990 (top graph), median of simulated mean daily survival through the Sacramento-San Joaquin River Delta, northern California (middle graph), and the difference in survival between the Proposed Action (PA) and No Action Alternative (NAA) scenarios (bottom graph). Heavy lines in the top graph show bypass discharge on the primary y-axis, and thin lines show DCC operation of open or closed on the second y-axis. In the bottom graph, the gray shaded region shows the 90% credible interval on the difference in survival between scenarios. Discharge in the top graph is shown on a logarithmic scale to highlight variation in discharge when discharge is low. C, Critical; WY, water year; ft^3/s, cubic foot per second; -, minus.

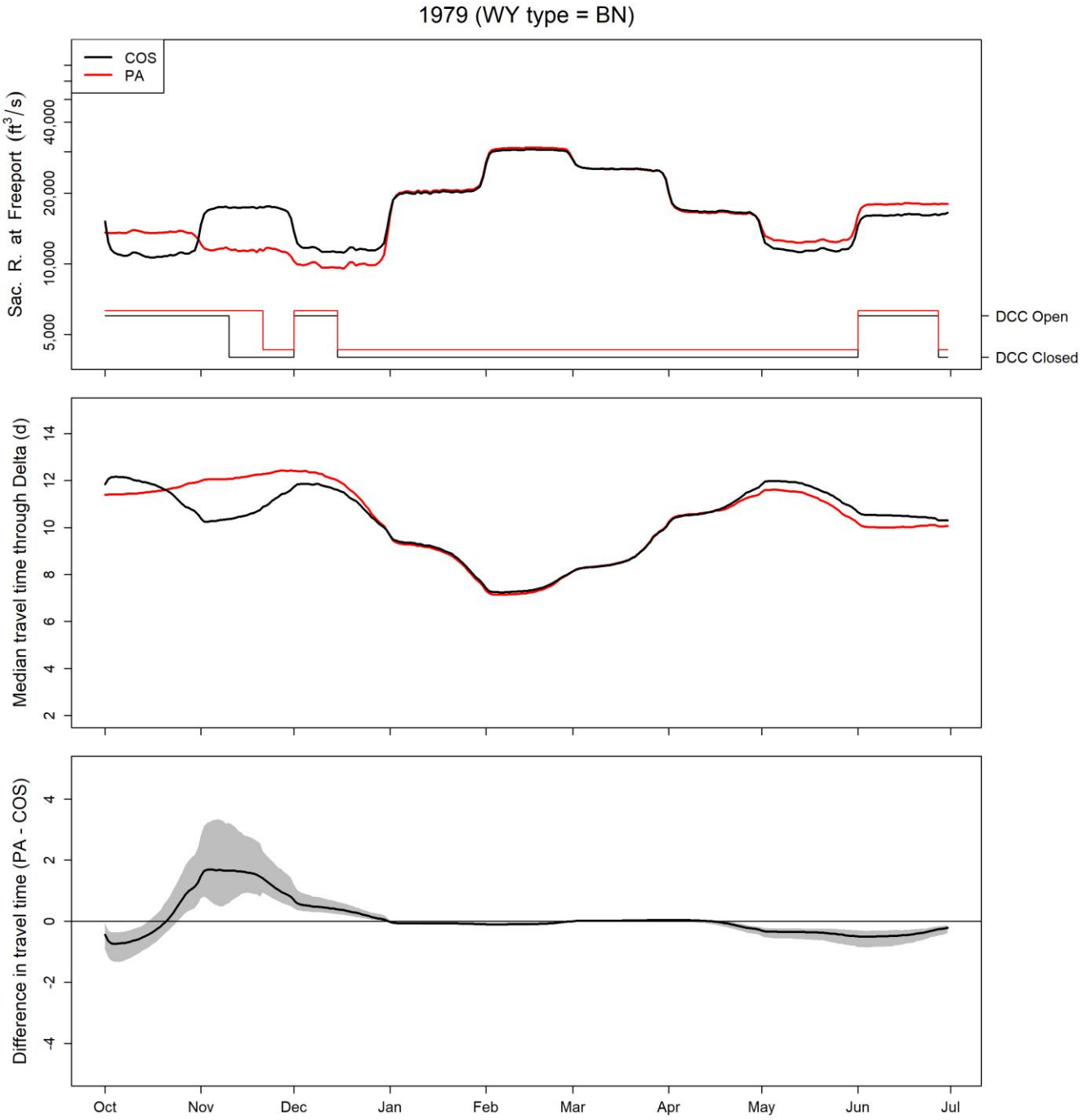

Figure 7. Graphs showing simulated daily bypass flows and Delta Cross Channel (DCC) gate operations for water year 1979 (top graph), simulated median daily travel time of juvenile Chinook salmon through the Sacramento-San Joaquin River Delta, northern California (middle graph), and the difference in travel time between the Proposed Action (PA) and No Action Alternative (NAA) scenarios (bottom graph). Heavy lines in the top graph show bypass discharge on the primary y-axis, and thin lines show DCC operation of open or closed on the second y-axis. In the bottom graph, the gray shaded region shows the 90% credible interval on the difference in median travel time between scenarios. Discharge in the top graph is shown on a logarithmic scale to highlight variation in discharge when discharge is low. BN, Below Normal; d, days; WY, water year; ft^3/s, cubic foot per second; -, minus.

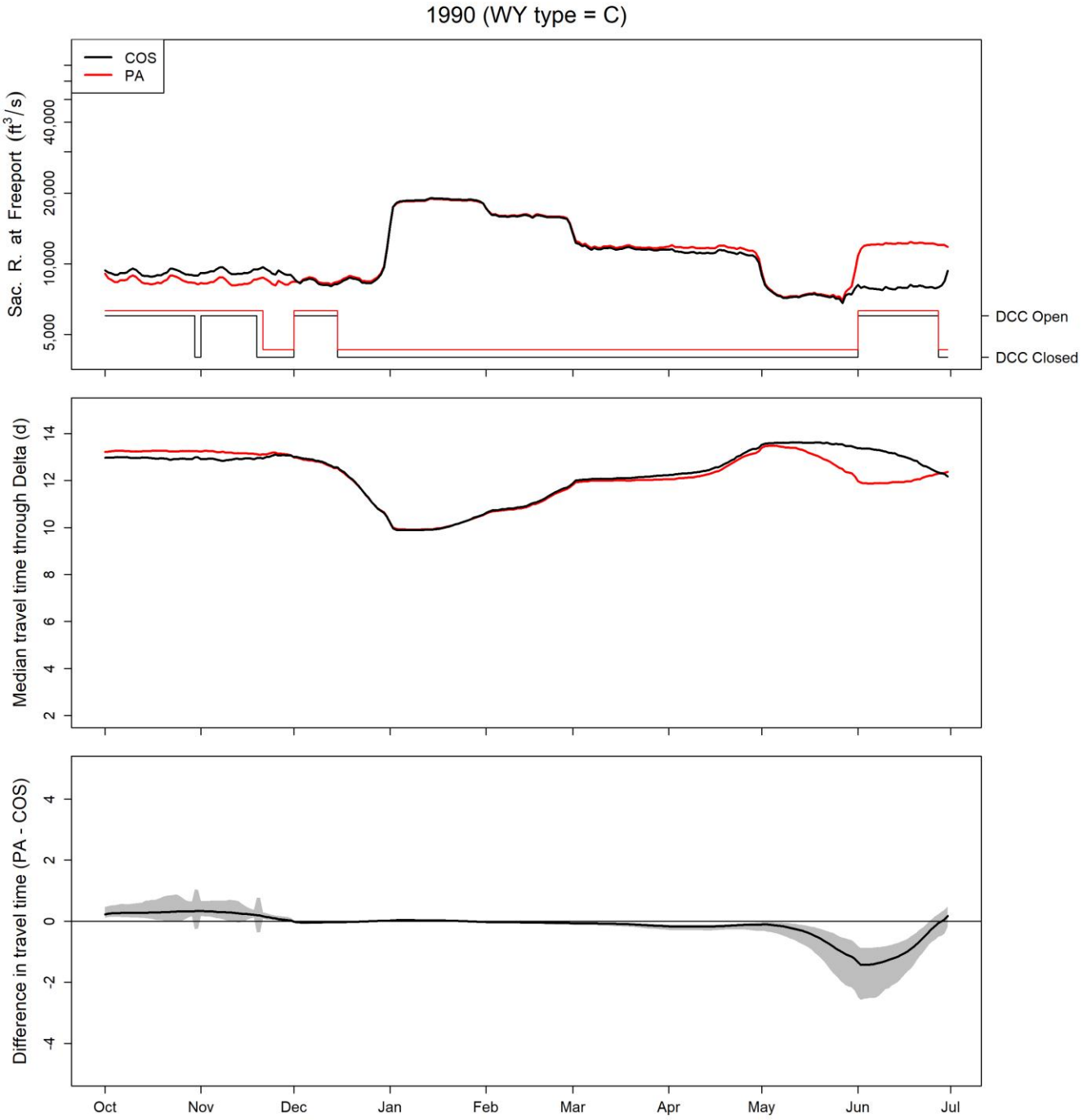

Figure 8. Graphs showing simulated daily bypass flows and Delta Cross Channel (DCC) gate operations for water year 1990 (top graph), simulated median daily travel time through the Sacramento-San Joaquin River Delta, northern California (middle graph), and the difference in travel time of juvenile Chinook salmon between the Proposed Action (PA) and No Action Alternative (NAA) scenarios (bottom graph). Heavy lines in the top graph show bypass discharge on the primary y-axis, and thin lines show DCC operation of open or closed on the second y-axis. In the bottom graph, the gray shaded region shows the 90% credible interval on the difference in median travel time between scenarios. Discharge in the top graph is shown on a logarithmic scale to highlight variation in discharge when discharge is low. C, Critical; d, days; WY, water year; ft^3/s, cubic foot per second; -, minus.

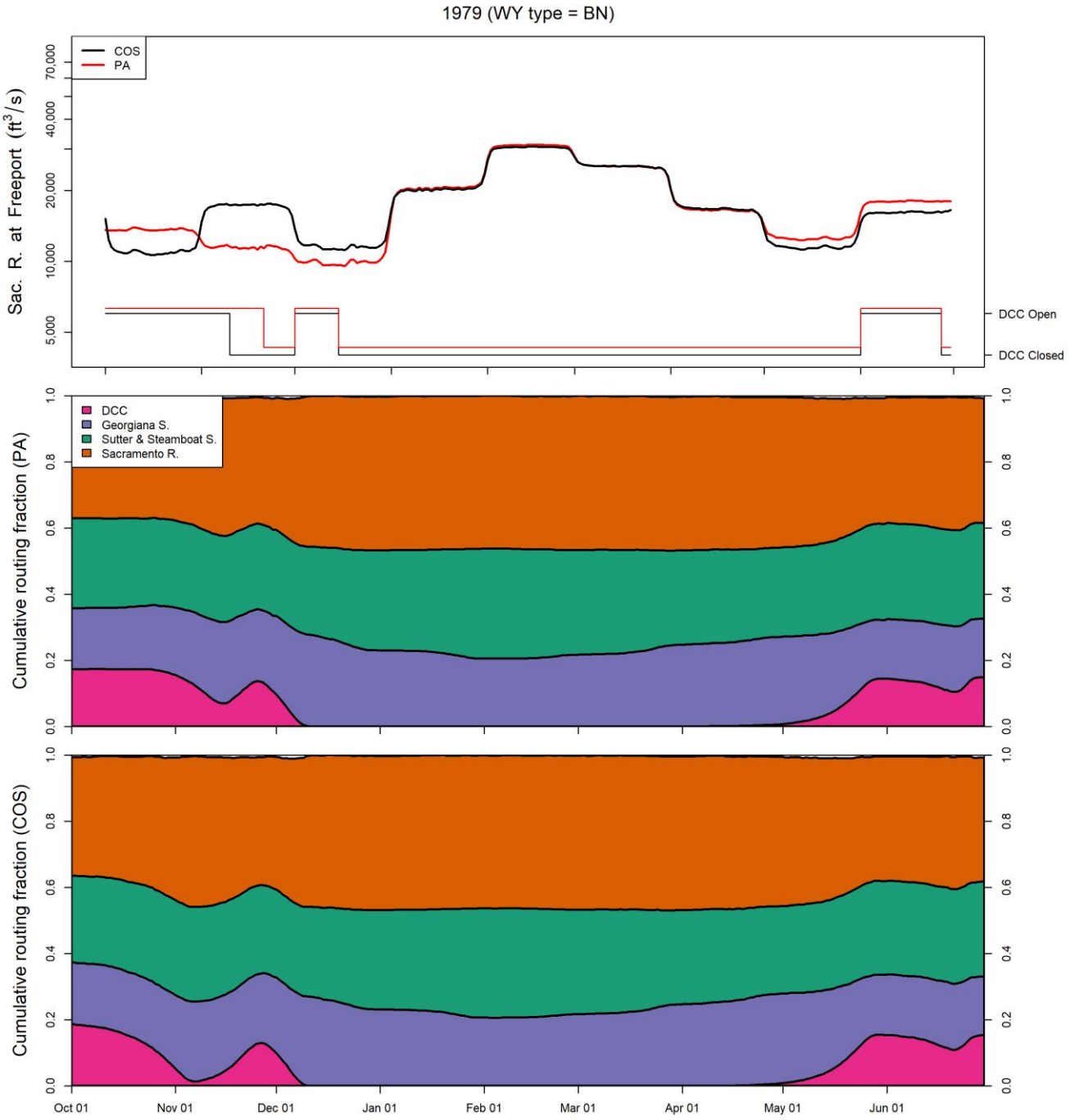

Figure 9. Graphs showing simulated daily bypass flows and Delta Cross Channel (DCC) gate operations for water year 1979 (top graph), and stacked line plots showing the daily cumulative migration route probabilities for the Proposed Action (PA, middle graph) and No Action Alternative (NAA, bottom graph) scenarios, Sacramento-San Joaquin River Delta, northern California. Heavy lines in the top graph show bypass discharge on the primary y-axis, and thin lines show DCC operation of open or closed on the second y-axis. Discharge in the top graph is shown on a logarithmic scale to highlight variation in discharge when discharge is low. C, Critical; WY, water year; ft^3/s, cubic foot per second.

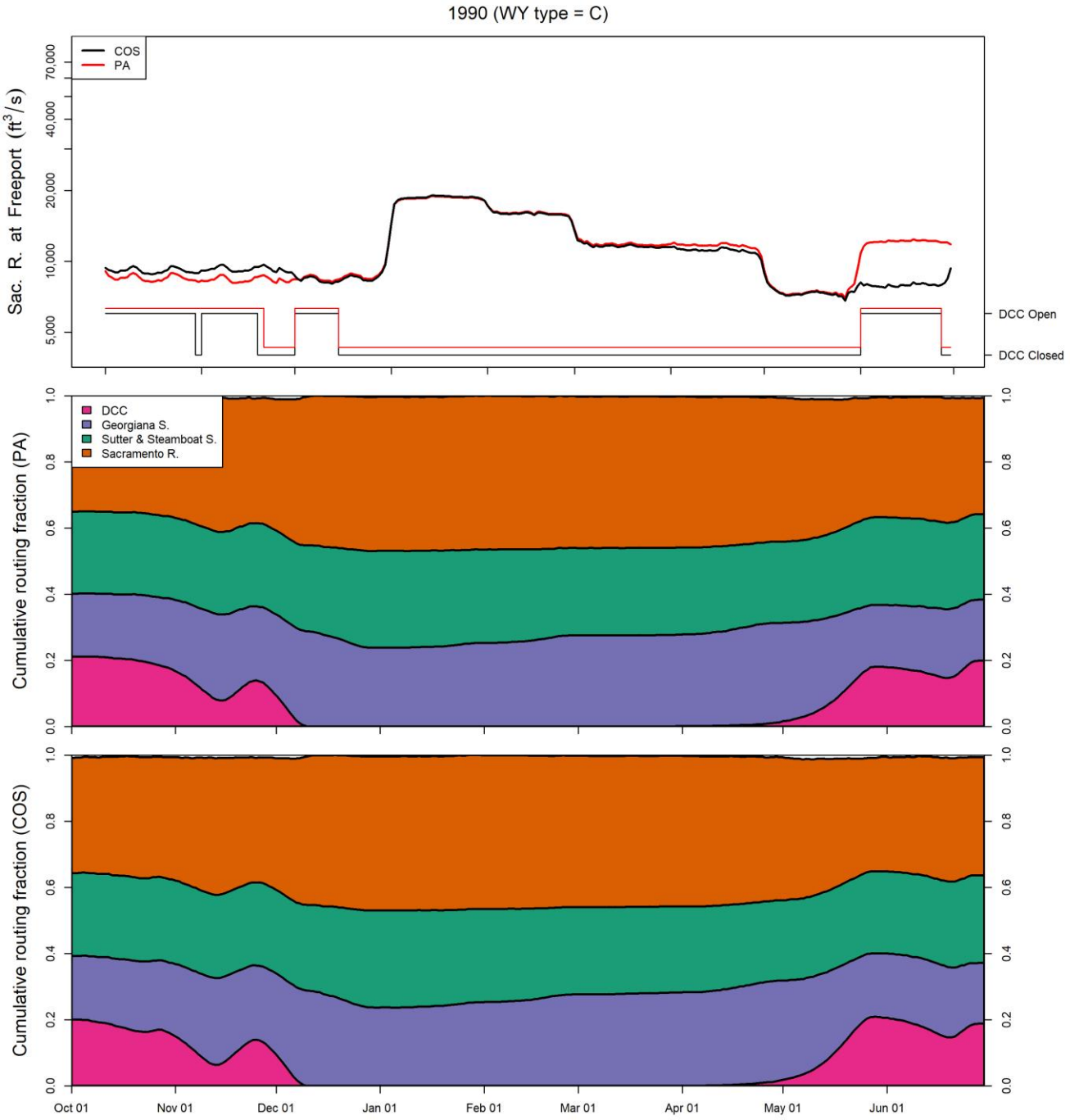

Figure 10. Graphs showing simulated daily bypass flows and Delta Cross Channel (DCC) gate operations for water year 1990 (top graph), and stacked line plots showing the daily cumulative migration route probabilities for the Proposed Action (PA, middle graph) and No Action Alternative (NAA, bottom graph) scenarios, Sacramento-San Joaquin River Delta, northern California. Heavy lines in the top graph show bypass discharge on the primary y-axis, and thin lines show DCC operation of open or closed on the second y-axis. Discharge in the top graph is shown on a logarithmic scale to highlight variation in discharge when discharge is low. BN, Below Normal; WY, water year; ft^3/s, cubic foot per second.

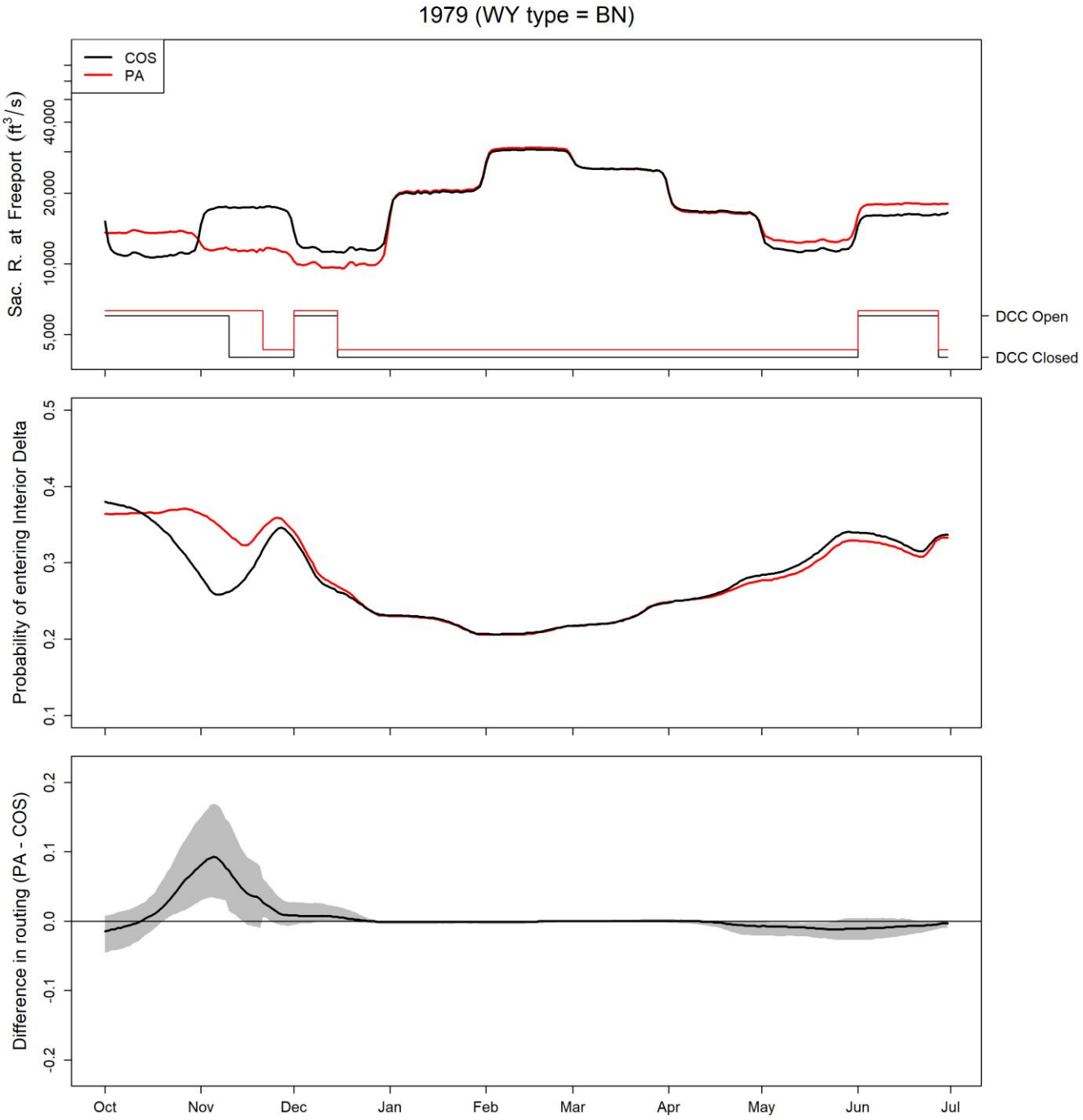

Figure 11. Graphs showing simulated daily bypass flows and Delta Cross Channel (DCC) gate operations for water year 1979 (top graph), simulated median route-specific travel time of juvenile Chinook salmon through the Sacramento-San Joaquin River Delta, northern California (middle graph), and the difference in route-specific travel time between the Proposed Action (PA) and No Action Alternative (NAA) scenarios (bottom graph). Heavy lines in the top graph show bypass discharge on the primary y-axis, and thin lines show DCC operation of open or closed on the second y-axis. Discharge in the top graph is shown on a logarithmic scale to highlight variation in discharge when discharge is low. BN, Below Normal; WY, water year; ft^3/s, cubic foot per second; -, minus.

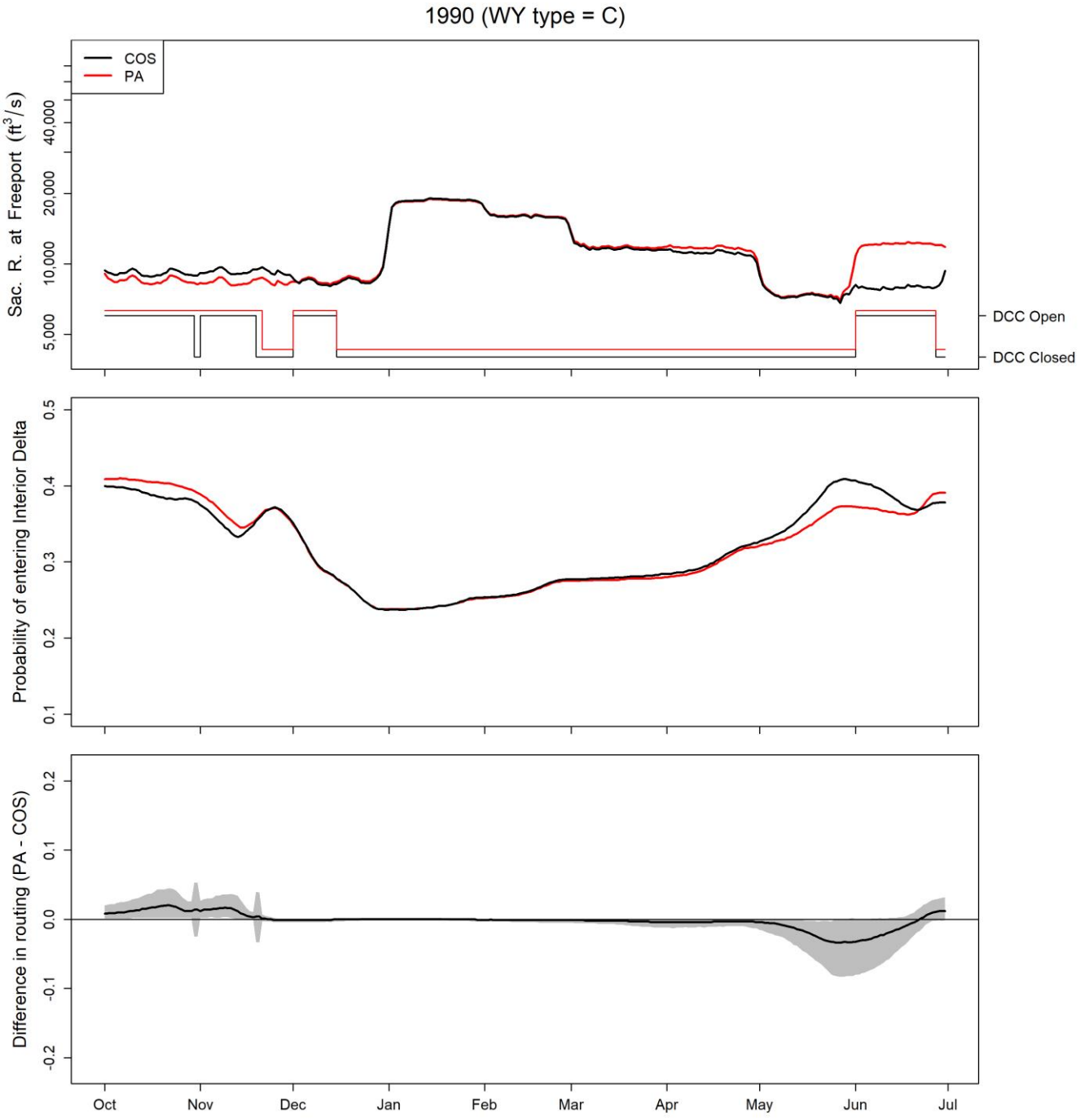

Figure 12. Graphs showing simulated daily bypass flows and Delta Cross Channel (DCC) gate operations for water year 1979 (top graph), median of simulated mean route-specific survival through the Sacramento-San Joaquin River Delta, northern California (middle graph), and the difference in route-specific survival between the Proposed Action (PA) and No Action Alternative (NAA) scenarios (bottom graph). Heavy lines in the top graph show bypass discharge on the primary y-axis, and thin lines show DCC operation of open or closed on the second y-axis. Discharge in the top graph is shown on a logarithmic scale to highlight variation in discharge when discharge is low. BN, Below Normal; WY, water year; ft^3/s, cubic foot per second; -, minus.

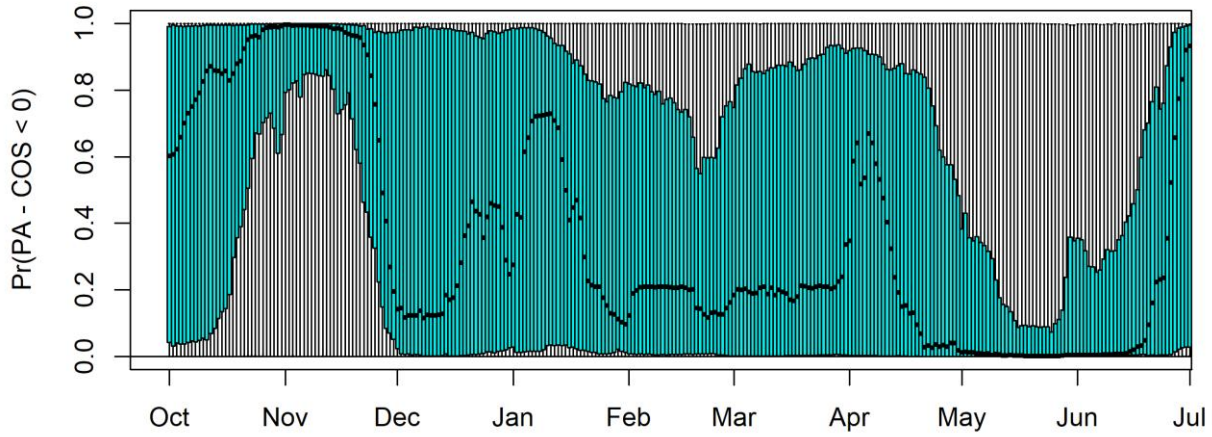

Figure 13. Boxplots showing the distribution of the probability that through-Delta survival for the PA scenario is less than survival for COS. Each box plot represents the distribution among years for a given date of the probability that the difference between PA and COS is less than zero. The point in each box represents the median, the box hinges represent the 25th and 75th percentile, and the whiskers display the minimum and maximum. Pr, probability; <, less than; -, minus.

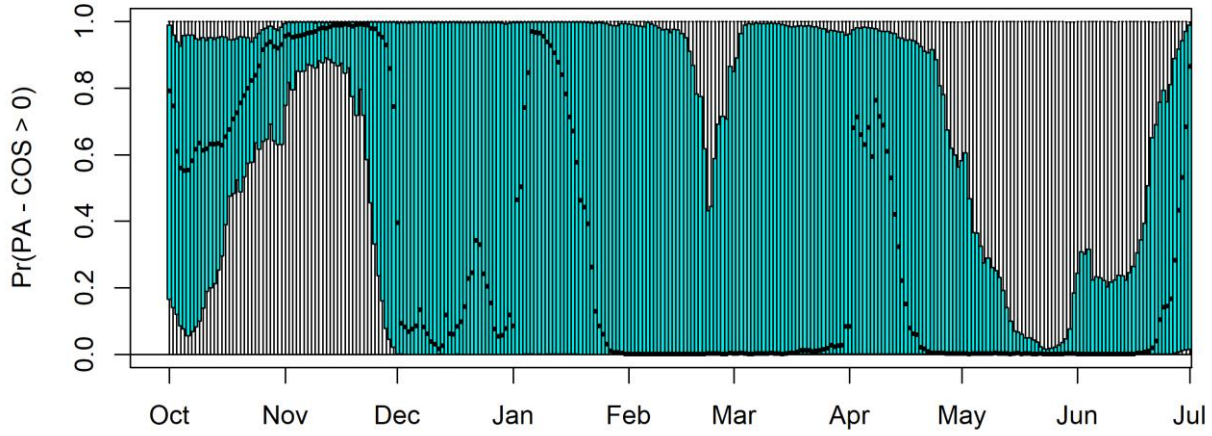

Figure 14. Boxplots showing the distribution of the probability that the difference in median travel time through the Delta between the COS and PA scenario is greater than zero. Each box plot represents the distribution among years for a given date of the probability that the difference between PA and COS is greater than zero. The point in each box represents the median, the box hinges represent the 25th and 75th percentile, and the whiskers display the minimum and maximum. Pr, probability; >, greater than; -, minus.

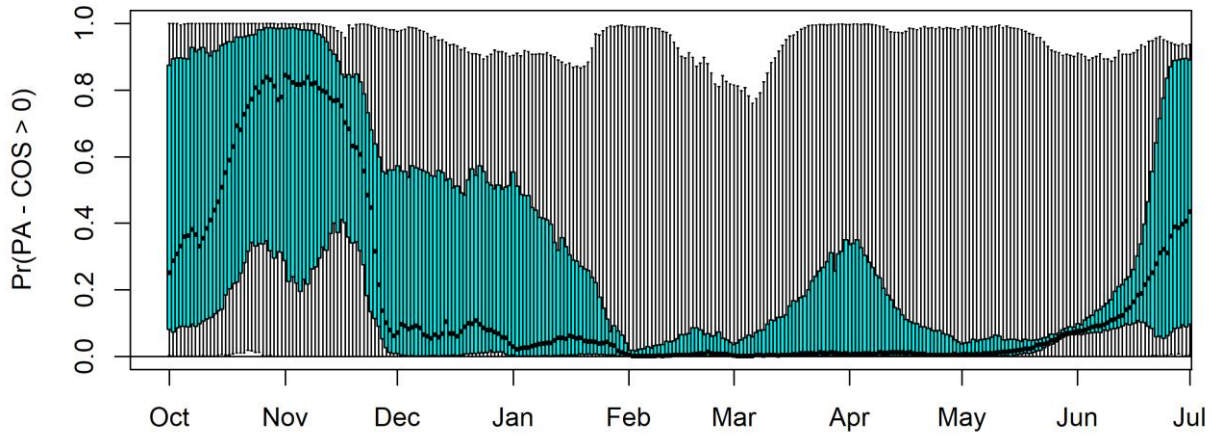

Figure 15. Boxplots showing the distribution of the probability that the difference in routing into the Interior Delta between the COS and PA scenario is greater than zero Each box plot represents the distribution among years for a given date of the probability that the difference between PA and COS is greater than zero. The point in each box represents the median, the box hinges represent the 25th and 75th percentile, and the whiskers display the minimum and maximum. Pr, probability; >, greater than; -, minus.

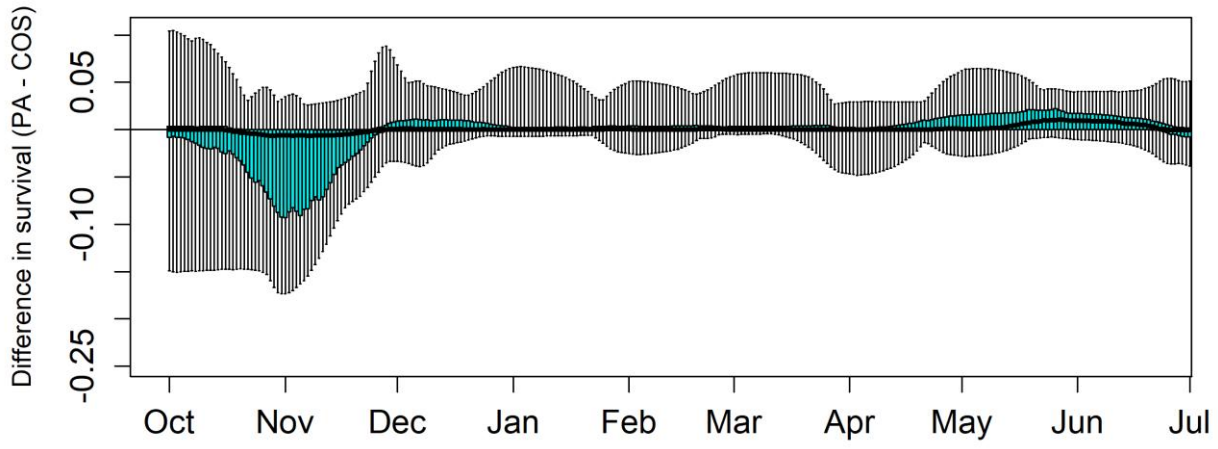

Figure 16. Boxplots of daily median differences in through-Delta survival between the PA and COS scenario. Each box plot represents the distribution of median survival differences among years for a given date. The point in each box represents the median, the box hinges represent the 25th and 75th percentile, and the whiskers display the minimum and maximum. -, minus.

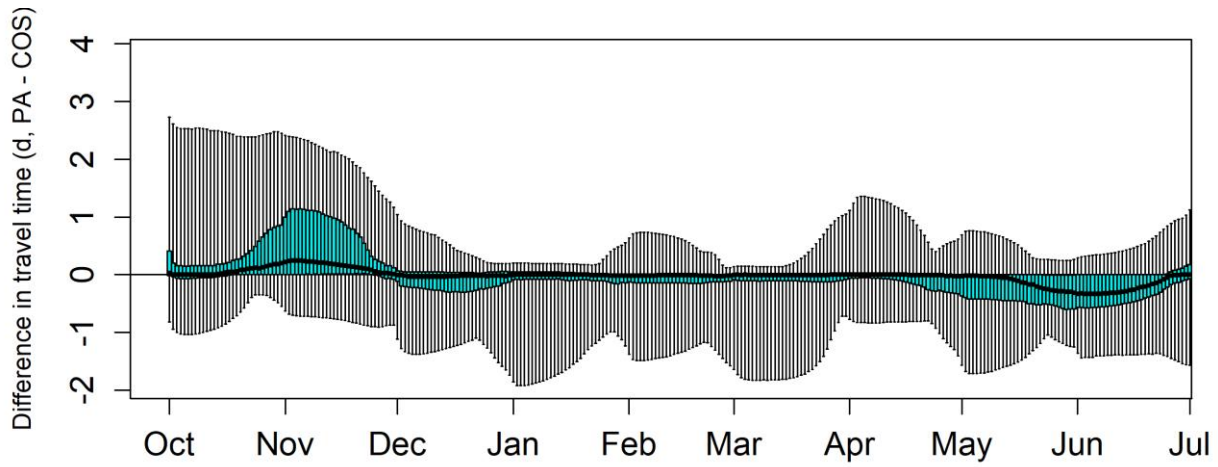

Figure 17. Daily boxplots of median differences in median travel time between the PA and COS scenario. Each box plot represents the distribution of median travel time differences among years for a given date. The point in each box represents the median, the box hinges represent the 25th and 75th percentile, and the whiskers display the minimum and maximum. d, days; -, minus.

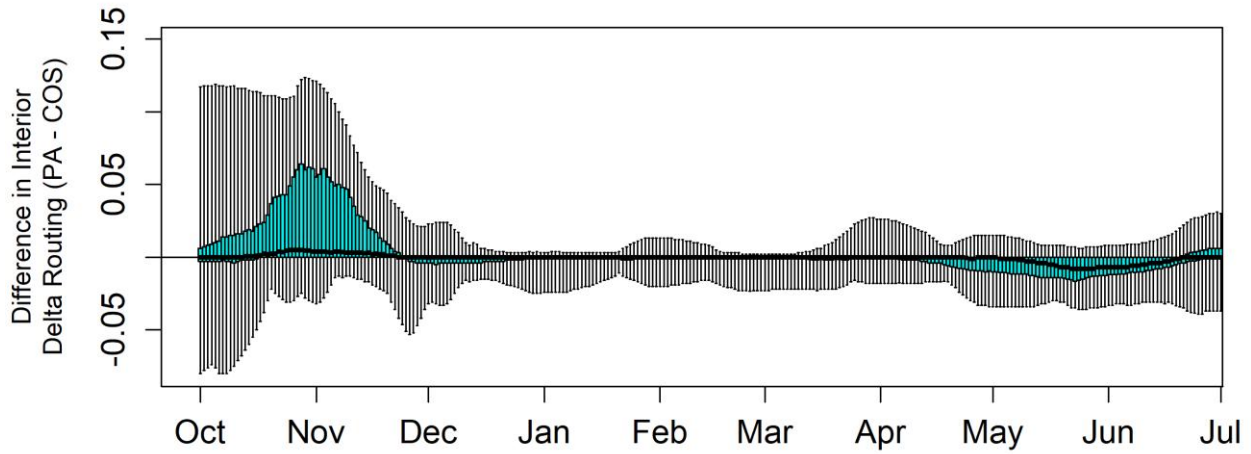

Figure 18. Daily boxplots of median differences in routing to the Interior Delta betwen the PA and COS scenario. Each box plot represents the distribution of median routing differences among years for a given date. The point in each box represents the median, the box hinges represent the 25th and 75th percentile, and the whiskers display the minimum and maximum. -, minus.

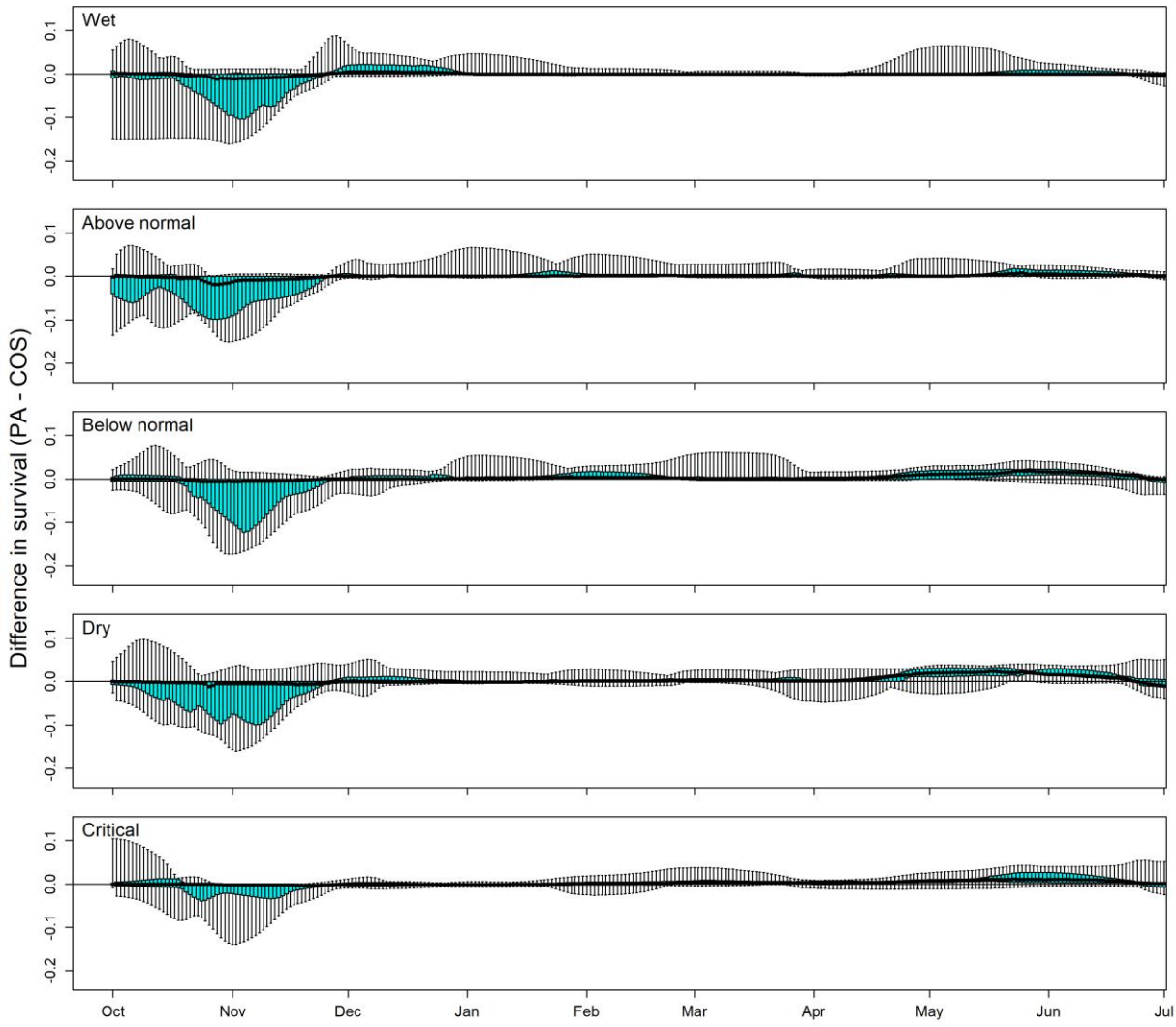

Figure 19. Daily boxplots of median differences in median through-Delta survival between the PA and COS scenario by water year type. Each box plot represents the distribution of median survival differences among years for a given date. The point in each box represents the median, the box hinges represent the 25th and 75th percentile, and the whiskers display the minimum and maximum. -, minus.

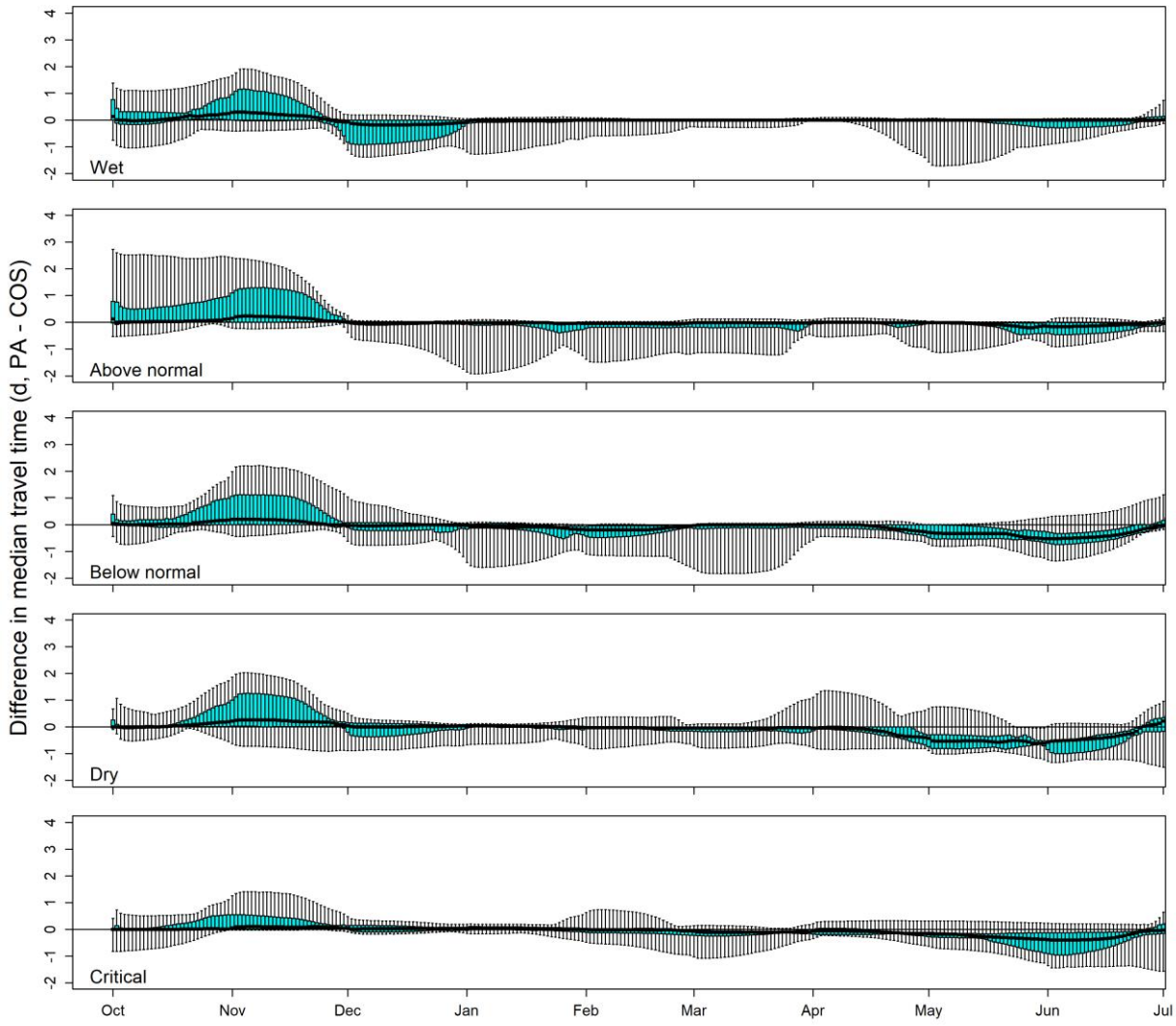

Figure 20. Daily boxplots of median differences in median travel time between the PA and COS scenario by water year type. Each box plot represents the distribution of median travel time differences among years for a given date. The point in each box represents the median, the box hinges represent the 25th and 75th percentile, and the whiskers display the minimum and maximum. d, days; -, minus.

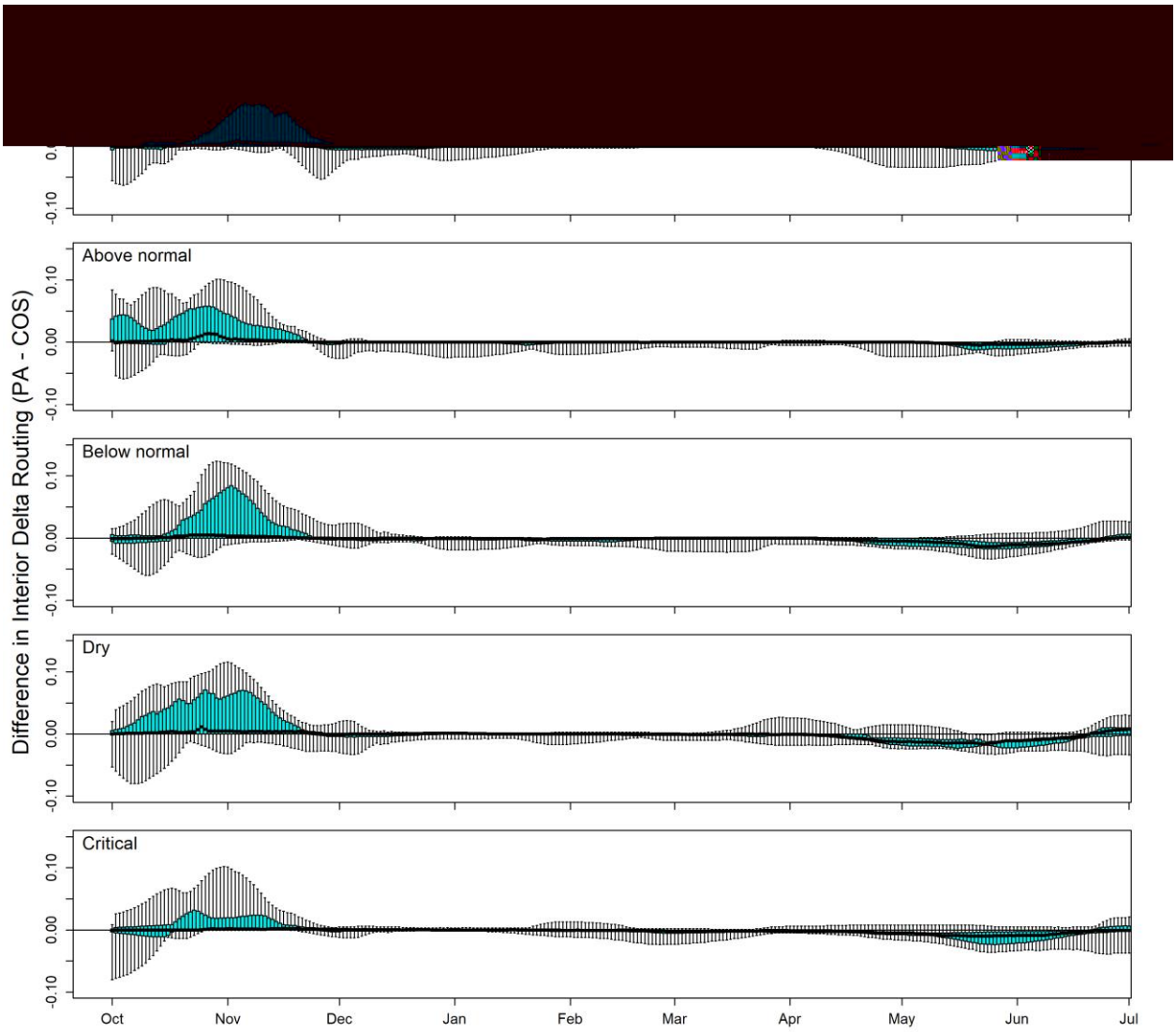

Figure 21. Daily boxplots of median differences in median travel time between the PA and COS scenario by water year type. Each box plot represents the distribution of median travel time differences among years for a given date. The point in each box represents the median, the box hinges represent the 25th and 75th percentile, and the whiskers display the minimum and maximum. d, days; -, minus.

References Cited

ICF International, 2016, Biological assessment for the California WaterFix: Prepared for the Bureau of Reclamation, Sacramento, California, ICF 00237.15., 62 p.

Kapahi, G., Baer, I., Farwell, J., Riddle, D., and Wilson, G., 2006, Water quality control plan for the San Francisco Bay/Sacramento-San Joaquin Delta Estuary: Sacramento, California, State Water Resources Control Board, 49 p.

King, R., Morgan, B., Gimenez, O., and Brooks, S., 2010, Bayesian analysis for population ecology: Boca Raton, Florida, CRC Press, 456 p.

Michel, C.J., Ammann, A.J., Lindley, S.T., Sandstrom, P.T., Chapman, E.D., Thomas, M.J., Singer, G.P., Klimley, A.P., and MacFarlane, R.B., 2015, Chinook salmon outmigration survival in wet and dry years in California's Sacramento River: Canadian Journal of Fisheries and Aquatic Sciences, v. 72, no. 11, p. 1749–1759, https://doi.org/10.1139/cjfas-2014-0528.

National Marine Fisheries Service (NMFS). 2009. Biological opinion and conference opinion on the longterm operations of the Central Valley Project and State Water Project. National Marine Fisheries Service Southwest Region, 844 p. accessed May 29, 2019, at https://www.westcoast.fisheries.noaa.gov/central_valley/water_operations/ocap.html.

Newman, K.B., 2003, Modelling paired release–recovery data in the presence of survival and capture heterogeneity with application to marked juvenile salmon: Statistical Modelling, v. 3, no. 3, p. 157–177, https://doi.org/10.1191/1471082X03st055oa.

Newman, K.B., and Rice, J., 2002, Modeling the survival of Chinook salmon smolts outmigrating through the lower Sacramento River system: Journal of the American Statistical Association, v. 97, no. 460, p. 983–993, https://doi.org/10.1198/016214502388618771.

Newman KB, Brandes PL. 2010. Hierarchical modeling of juvenile Chinook salmon survival as a function of Sacramento-San Joaquin Delta water exports. N Am J Fish Manag 30:157–169. doi: http://dx.doi.org/10.1577/M07-188.1

Perry, R.W., 2010, Survival and migration dynamics of juvenile Chinook salmon (*Oncorhynchus tshawytscha*) in the Sacramento-San Joaquin River Delta: Seattle, University of Washington, School of Aquatic and Fishery Sciences, Ph.D. dissertation, 223 p.

Perry, R.W., Brandes, P.L., Burau, J.R., Klimley, A.P., MacFarlane, B., Michel, C., and Skalski, J.R., 2013, Sensitivity of survival to migration routes used by juvenile Chinook salmon to negotiate the Sacramento-San Joaquin River Delta: Environmental Biology of Fishes, v. 96, nos. 2–3, p. 381–392, https://doi.org/10.1007/s10641-012-9984-6.

Perry, R.W., Pope, A.C., Romine, J.G., Brandes, P.L., Burau, J.R., Blake, A.R., Ammann, A.J., and Michel, C.J., 2018, Flow-mediated effects on travel time, routing, and survival of juvenile Chinook salmon in a spatially complex, tidally forced river delta: Canadian Journal of Fisheries and Aquatic Sciences, https://doi.org/10.1139/cjfas-2017-0310.

Perry, R.W., Skalski, J.R., Brandes, P.L., Sandstrom, P.T., Klimley, A.P., Ammann, A., and MacFarlane, B., 2010, Estimating survival and migration route probabilities of juvenile Chinook salmon in the Sacramento-San Joaquin River Delta: North American Journal of Fisheries Management, v. 30, no. 1, p. 142–156, https://doi.org/10.1577/M08-200.1.

Reclamation, 2019, Reinitiation of Consultation on the Coordinated Long-Term Operation of the Central Valley Project and State Water Project: Final Biological Assessment, 871 p., accessed May 29, 2019, at https://www.usbr.gov/mp/bdo/lto.html.

Appendixes

Appendixes 1–4 are Adobe Acrobat® files and are available for download at https://doi.org/10.3133/ofr2019XXXX.

Appendix 1. Simulated Daily Survival by Year, Continuing Operations Compared to Proposed Action Scenarios, 1922–2003

Appendix 2. Simulated Daily Travel Time by Year, Continuing Operations Compared to Proposed Action Scenarios, 1922–2003

Appendix 3. Simulated Daily Routing by Year, Continuing Operations Compared to Proposed Action Scenarios, 1922–2003

Appendix 4. Simulated Proportion of Fish Entering the Interior Delta by Year, Continuing Operations Compared to Proposed Action Scenarios, 1922–2003